MOMENT–ROTATION RELATIONSHIPS OF NON-BONDED POST-TENSIONED I- AND T-BEAMS

Edward G. Nawy
Professor of Civil Engineering
Rutgers—The State University of New Jersey
New Brunswick, New Jersey

Franklin Salek
Assistant Professor of Civil Engineering
Newark College of Engineering
Newark, New Jersey

Limit behavior of concrete structures is being emphasized more frequently today. In steel structures it is an accepted method of analysis and design; in reinforced concrete, extensive work has already been done on evaluation of the rotational capacity of the plastic hinges and quantitative recommendations are being considered for the next revision of the American Concrete Institute's *Building Code Requirements for Reinforced Concrete* (ACI 318-63).

In prestressed concrete, however, further extensive research is needed to study the rotation of the plastic hinge and the resulting favorable moment redistribution. With the increased use of prestressed concrete in continuous structures, logical and economical designs can be achieved by applying limit methods.

Therefore, this study investigates the possibility of increasing the rotational capacity of prestressed concrete members by introducing continuous rectangular spiral binders at the critical sections of the beams. The research is part of a cooperative program with Commission XI of the European Concrete Committee.

The major parameter varied was the spiral percentage, p''. The tests conducted were restricted to non-bonded, post-tensioned beams. The use of non-bonded strands will be compared with the behavior of bonded pretensioned strands in the program's second stage.

NOTATION

b = width of section
h = depth of section
L_1 = point on the moment-rotation diagram where elastic behavior ceases
L_2 = point on the moment-rotation diagram where reasonably ideal plasticity is developed
f'_c = cylinder compressive

The results from tests using post-tensioned, non-bonded, I- and T-beams are analysed to determine the contribution of variable amounts of continuous confining spiral binders to the magnitude of rotation of plastic hinges in prestressed concrete structures.

strength of concrete
f'_t = tensile splitting strength of concrete
f_y = yield strength of steel
f_u = ultimate strength of steel
f_e = effective prestressing stress
M = moment at any loading stage
M_y = moment at L_1
M_u = ultimate moment
X_2h = depth of the compressive zone
p'' = rectangular spiral binders percentage by volume

TEST SPECIMENS

Geometric Properties. The dimensions of the I- and T-sections are shown in Fig. 1. The main prestressing reinforcement for the I-beams is four ¼-in., seven-wire strands, three in the flange and one in the web. The main prestressing reinforcement for the T-beams is five ¼-in., seven-wire strands located in the web. The effective span length of each beam was 7 ft. 6 in. and the total length of each beam, 8 ft. 1½ in.

The concrete mix proportions were 6.5 sacks of high early strength cement, 1580 lb. of graded sand, 1850 lb. of graded ¾-in. crushed stone and a total of 35 gal. of water per cubic yard of concrete.

The spiral binders were fabricated of No. 11-gage high strength 0.1205 in. diameter wire; stirrups of the same material had a diameter of 0.25 in. They had a yield strength of $f_y = 89.3$ ksi and an ultimate strength, $f_u = 95$ ksi.

The cross-sectional area of the ¼-in. strands was 0.036 sq. in. The strands had a yield strength of $f_y = 225$ ksi and an ultimate strength, $f_u = 278$ ksi*. The effective stress f_e was 167 ksi in all tests except I1T0

Values are test values. Catalog values are: $f_y = 215$ ksi; $f_u = 253$ ksi.

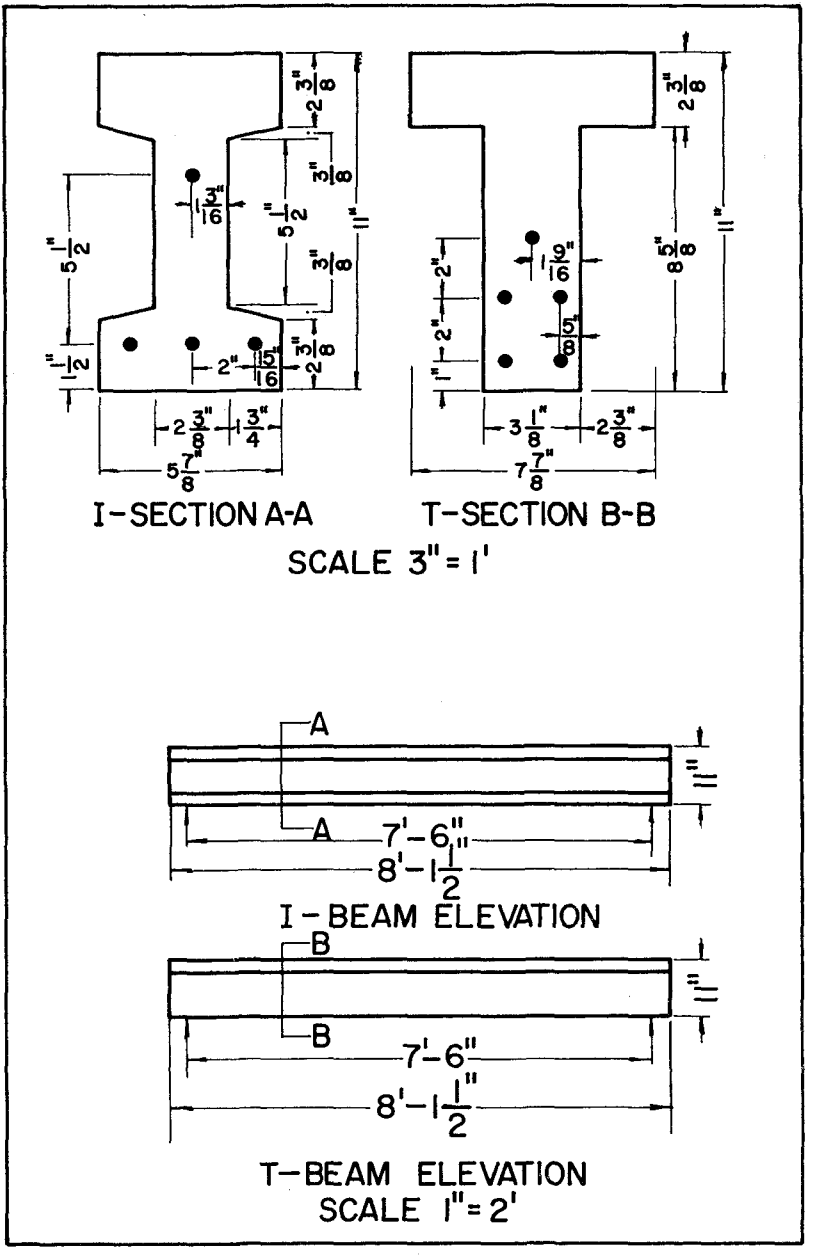

Fig. 1. Geometric properties of beams

and T3T2 where f_e was 111 ksi.

The stress-strain diagrams for the rectangular spiral binders and the prestressing strands are shown in Figs. 2 and 3.

The ducts for the prestressing strands were No. 12 polyethylene tubing having a ⅜-in. inside diameter and a ½-in. outside diameter. The end grips for the prestressing strands were ¼-in. Supreme strand chucks. The spiral binders were 28-in. long and located at the central segment of each beam extending 14 in. to either side of the centerline. The dimensions are shown in Fig. 4. The percentage of spiral p'' was the variable parameter ranging from 2 percent with a 1-in. pitch to zero (see Fig. 5 for spiral at 1-in. spacing and Fig. 6 for 3-in. spacing). Open rectangular stirrups at 6-in. spacing provided shear reinforcement where there was no spiral reinforcing (Fig. 7). The rectangular spirals binding the whole concrete section were chosen because they also serve as shear reinforcement.

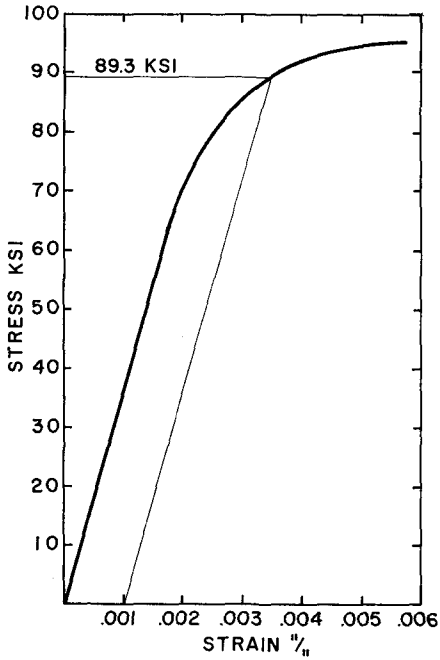

Fig. 2. Stress-strain diagram for the spiral steel

Instrumentation. The prestressing strands were difficult to instrument as each strand consisted of seven individual wires. SR-4 type A-12 strain gages were used with the felt backing removed and the gage trimmed to minimum width. Because of the small size of the wire, the trimmed gage was preformed by wrapping it around a wire and holding it with an elastic band for 24 hours before permanent mounting. The preformed gage was then fastened with Duco Cement on the cleaned strand wire, wrapped with an elastic band and cured for 48 hours. After curing, electrical leads were soldered and the gage fully water-proofed. SR-4 type A-7 strain gages were used on the spiral binders.

To record the compressive strain at the extreme top fibers of the concrete, SR-4 type A-3 strain gages were placed on the top surface of the beams on either side of the loading platten. To record the strain in the concrete beam over its depth, four rows of demountable mechanical gage discs (DEMEC) were mounted at a gage spacing of 4 in. in the central 32-in. portion of the span and 8 in. at the two outer portions as shown in Fig. 8. The DEMEC gages had an accuracy of 1×10^{-5} in./in. Budd adhesive, type CA-1, with a curing rate of 30 seconds, was used to mount the discs on the prepared concrete surface. Eight inclinometers, used to determine direct rotation, were located on the top of the beams (Fig. 9). They have a bubble sensitivity

Table 1. Properties of test beams

Beam	d in.	h in.	Test age days	f'_c psi	f'_t psi	No. of strands	Prestress A_s sq. in.	Spiral pitch in.	Spiral p'' %
I1T0	8.125	11	45	6313	744	4	.144	—	0.00
I2T1	8.125	11	15	5013	566	4	.144	1	2.00
I3T2	8.125	11	21	5517	588	4	.144	2	1.00
I4T3	8.125	11	22	5429	526	4	.144	3	0.67
I5T4	8.125	11	22	5623	581	4	.144	4	0.50
I6T1	8.125	11	23	5500	548	4	.144	1	2.00
T1T0	8.4	11	52	6304	747	5	.180	—	0.00
T2T1	8.4	11	29	5783	526	5	.180	1	1.80
T3T2	8.4	11	24	5809	522	5	.180	2	0.90
T4T3	8.4	11	15	6419	588	5	.180	3	0.60
T5T4	8.4	11	26	5482	606	5	.180	4	0.45
T6T1	8.4	11	16	6419	584	5	.180	1	1.80

of 60 seconds per division. The properties of the test beams and the results of the control tests on the concrete cylinders and reinforcement are tabulated in Table 1.

TESTING PROCEDURE

Each beam was post-tensioned, using a Freyssinet jack, one day prior to testing. Readings of the SR-4 electric gages, the DEMEC gages and the inclinometers were taken before and after prestressing.

All beams were tested in a calibrated flexure hydraulic testing frame of load accuracy of 0.5 percent (see Fig. 9).

Each beam was supported by a hinge at one end and a roller at the other. Supports were 3¾ in. from either end of the beams. Load was applied at midspan on a 1½-in. strip by a pair of hydraulic jacks symmetrically placed above a load cell.

Electric strain indicators were used to read the SR-4 gages. The change in slope was read from the Mayes inclinometers. Central deflections were measured with Ames dials having an accuracy of 1/1000 and a travel of 2 in. The deflections were measured on the underside of the beams at the center and at 4 in. on either side of the center.

Strains measured on the lateral surfaces of the beams were obtained over 4- and 8-in. gage length DEMEC discs located in four rows with fifteen discs per row. The vertical spacing of the four rows was ¾ in. and 1¾ in. from the top of beam, at the neutral axis, and at the center of gravity of the prestressing steel.

Prior to loading, all readings were again taken. The loading applied in the elastic range consisted of three equal increments. When the elastic range was exceeded, it was necessary to set each of the loading stages by increments of deflection.

Load measurements were taken after each stage of application before any other readings were taken and immediately prior to the next incremental stage. Each loading stage lasted approximately 25 minutes. Application of each load increment took five minutes.

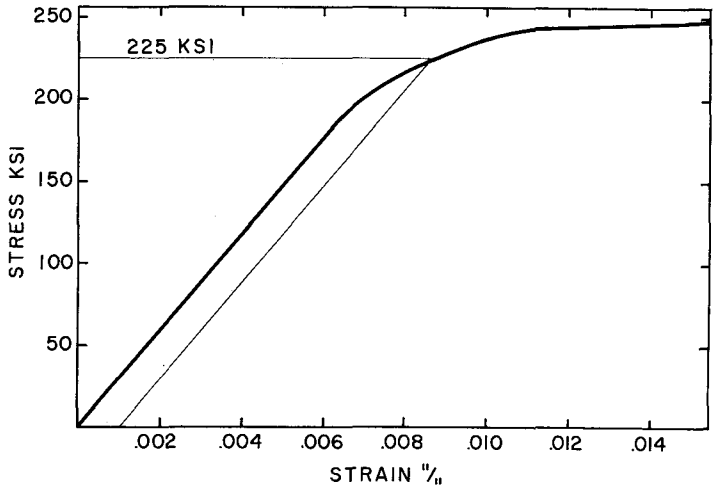

Fig. 3. Stress-strain diagram for the prestressing steel

Table 2. Yield and ultimate moments at midspan

Beam	M_y k-in.	M_u k-in.	M_y/M_u
I1T0	124.3	243.0	.512
I2T1	167.5	250.6	.669
I3T2	199.0	301.5	.662
I4T3	167.8	266.4	.630
I5T4	178.3	294.7	.605
I6T1	150.0	231.8	.649
T1T0	196.5	369.6	.532
T2T1	233.0	352.2	.663
T3T2	159.0	315.6	.503
T4T3	243.5	375.5	.649
T5T4	208.0	349.7	.597
T6T1	208.0	417.3	.498

TEST RESULTS

Behavior of Test Beams. The I- and T-beams both followed the same general pattern of behavior during the tests. For each type of beam rotations and deflections increased under increasing load from zero until the yield limit was reached. Then the rotations and deflections continued to increase with smaller increments of load until the ultimate load was reached, at which time rotations and deflections increased without any further increase in load.

All beams developed a single crack at midspan in the region of maximum moment. The crack, once developed, progressed very rapidly under successive load increments into the top flange of the beam.

Once the crack entered the top flange and reduced the depth of the compressive zone of the critical section, subsequent load increments caused the compressive zone to fail by crushing. The critical section was located at the position of maximum moment which, for the simply supported beam, was its midspan. This behavior is consistent with results reported by Janney, Hognestad, and McHenry[1].

Moment Ratios. The ratio of the yield moments to the ultimate moments for the I-beams varied from 0.512 to 0.669 with an average value of 0.621. For the T-beams this ratio varied from 0.498 to 0.663 with an average value of 0.574 (see Table 2).

Moment-Curvature Characteristics. Up to the L_1 limit the curvatures were uniformly distributed along the length of the beam. Initially the curvatures were negative due to the negative bending moment caused by the eccentric prestress force. As the load increments were applied the curvatures at the center became positive and remained uniformly distributed.

When the L_1 limit was reached, the curvatures over the two center 4-in. gage lengths rose sharply. The curvature distribution over the remaining portion of the beams increased uniformly. In general, one of the two center gages indicated a much larger curvature than the

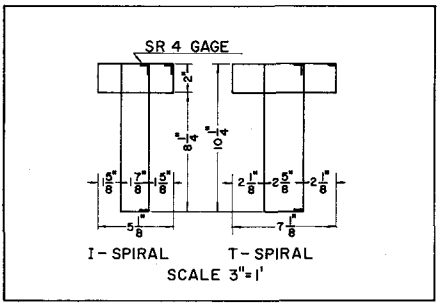

Fig. 4. Dimensions of spiral binders

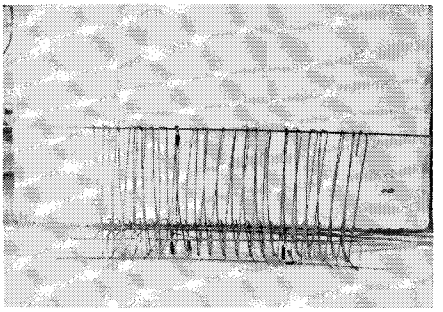

Fig. 5. Spiral binders at 1 in. spacing

other.

The test results point out that the curvature is uniformly distributed along the length of the beam up to the L_1 limit. Once the L_1 limit is exceeded, the curvature becomes concentrated at the critical section and increases very rapidly as the moment increases. There was only a slight increase in the magnitude of the curvature over the remaining portions of the beam.

The maximum values of curvature at midspan at the L_1 limit for the I-beams varied from 3.75×10^{-5} radians per in. for 2 percent spiral binders to 2.50×10^{-5} radians per in. without binders. The maximum values of curvature at midspan for the T-beams varied from 5.20×10^{-5} radians per in. for 2 percent binders to 3.10×10^{-5} radians per in. without binders.

It was necessary to obtain the curvature distribution along the beams so that the total beam rotation between the supports could be computed. The curvature distribution was also necessary for evaluation of the equivalent plastic hinge length.

The curvature at the beam ends was negative due to the negative moment produced by the eccentric prestressing force and was present throughout the entire range of loading because the applied load did not cause any change in moment at the supports.

Moment-Rotation Characteristics. For proper data interpretation, idealization of the moment-rotation relationship was made into a three stage behavior (Fig. 11). On the moment-rotation diagram two limits were defined by the changing behavior of the beam under increasing load. The L_1 limit, or the yield limit, is the point on the diagram where elastic behavior ceased; the L_2 limit is the point where reasonably ideal plasticity developed.

As tabulated in Table 3, the rotations at yield for the I-beams varied from 0.000025 to 0.001766 radians and had an average value of 0.000680 radians. The rotations at yield for the T-beams varied from −0.002133 to 0.00286 radians and had an average value of 0.000639 radians.

The rotations at L_2 for the I-beams varied from 0.039215 to 0.072931 radians and had an average value of 0.050453 radians. The rotations for the T-beams varied from 0.047224 to 0.070437 radians and had an average value of 0.056172 radians. Plots of the actual moment-rotation relationships are shown in Figs. 12 and 13. The difference between the ro-

tation at L_1 and at L_2 is the plastic rotation of the beam. These rotations averaged 0.049772 radians for the I-beams and 0.055533 radians for the T-beams.

The moment-rotation relationship does not apply to any one section of the beam but to the entire length of the beam. The moment referred to was the ratio of M/M_u with both M and M_u measured at midspan. The rotation was the total angle change measured between supports at each stage of loading including inelastic rotation at advanced loading stages. The moment-rotation curves for all the beams have the same general appearance. Each diagram has three phases: 1. The elastic phase, characterized by a linear relationship between moment and rotation, that rises almost vertically and terminates at about 60 percent of the ultimate load observed by appearance of the first crack. 2. The inelastic phase that starts at the end of the elastic phase, rises gradually and terminates at the ultimate load. 3. The ultimate phase, characterized by the horizontal portion of the graph.

The slope of the elastic phase for both types of beams is almost the same (compare Fig. 12 with Fig. 13). However, the rotation at zero load and the L_1 limit for both groups of beams differed. The moment-rotation behavior was not affected by the change in percentage of spiral binders.

Strain values in the concrete were analyzed to determine whether or not there were any limiting values associated with the elastic range of behavior. The concrete strains varied from 0.0215 to 0.0498 percent for the I-beams and from 0.0282 to 0.0626 percent for the T-beams. These strain values are considerably less than the value of 0.2 percent for bonded prestressed concrete beams as proposed by the European Concrete Committee.

At the L_2 limit the concrete strains varied from 0.414 to 0.805 percent for the I-beams and from 0.553 to 1.08 percent for the T-beams. These values are higher than the value of 0.35 percent for the bonded prestressed members proposed by the European Concrete Committee. The

Table 3. Midspan deflections and total rotations

Beam	M_y/M_u	Deflection in.		Rotation radians		Plastic rotation radians	X_2h in.
		L_1	L_2	L_1	L_2		
I1T0	.512	.099	1.017	.001766	.042127	.040361	.87
I2T1	.669	.075	1.764	.000399	.057683	.057284	.95
I3T2	.662	.045	1.043	.000766	.046125	.045359	.85
I4T3	.630	.054	1.041	.000561	.044634	.044073	.89
I5T4	.605	.061	0.915	.000025	.039215	.039190	.82
I6T1	.649	.062	1.696	.000564	.072931	.072367	.89
T1T0	.532	.083	1.180	.002133	.047224	.049357	.90
T2T1	.663	.129	1.845	.001133	.063778	.062645	1.07
T3T2	.503	.109	1.386	.002866	.059515	.056649	.85
T4T3	.649	.105	1.209	.000433	.049756	.050189	.89
T5T4	.597	.121	1.140	.001299	.046325	.045026	.89
T6T1	.498	.084	1.959	.000101	.070437	.070336	.79

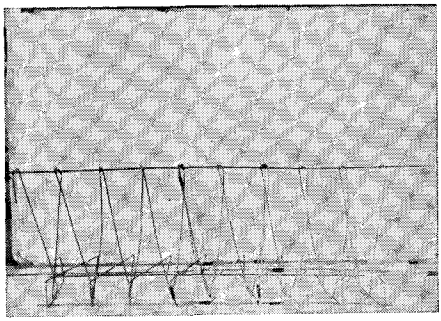

Fig. 6. Spiral binders at 3 in. spacing

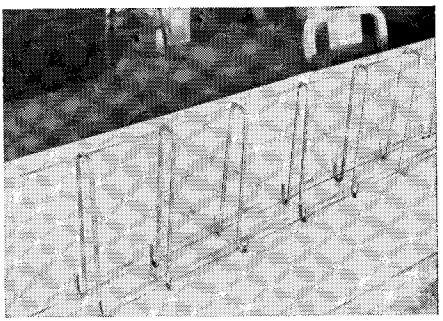

Fig. 7. Diagonal tension stirrups

concrete strains at the L_1 limit are low because the L_1 limit is defined by the cracking moment which is a function of the prestressing force. The concrete strains at the L_2 limit are high because of the lack of redistribution of stress in the unbonded member.

Midspan Deflection. The midspan deflections at the L_1 limit for the I-beams varied from 0.045 in. to 0.099 in. and had an average value of 0.066 in. The midspan deflections at the L_1 limit for the T-beams varied from 0.083 in. to 0.129 in. and had an average value of 0.105 in.

Diagrams for moment ratio M/M_u vs. midspan deflection were plotted for each beam (Figs. 14 and 15). The resulting curves were essentially similar in shape to those of the moment-rotation diagrams. The elastic portion of each diagram was a linear relationship up to approximately 60 percent of the ultimate load. The inelastic portion of the diagram was a gradually rising curve starting at the end of the elastic portion and terminating at ultimate load. The last portion of the diagram was horizontal and developed beyond ultimate load.

Table 4. Ratios of computed and observed values of moment

Beam	Cracking Moment M_y M(test)/M(calc)	Ultimate Moment M_u M(test)/M(calc)	p'' %
I1T0	0.935	0.840	0.00
I2T1	0.935	0.960	2.00
I3T2	1.110	1.150	1.00
I4T3	0.937	1.010	0.67
I5T4	1.000	1.130	0.50
I6T1	0.840	0.885	2.00
T1T0	0.975	1.050	0.00
T2T1	1.150	1.000	1.80
T3T2	1.040	0.900	0.90
T4T3	1.200	1.070	0.60
T5T4	1.030	1.190	0.45
T6T1	1.030	0.996	1.80
Mean	1.015	1.015	

Maximum deflections ranged from 1.38 to 2.64 in. for the I-beams and from 1.75 to 2.84 in. for the T-beams. These differences arose primarily from the ultimate phase of behavior when the beams exhibited arch action.

DISCUSSION

Analysis of the test results shows that the elastic limit of the beams was characterized by initial cracking of the beam rather than material failure in yielding of the prestressing steel because the cracking load is primarily a function of the prestressing force. Since the beams investigated in this program are underreinforced, one would expect the elastic limit to be set by yielding of the prestressing strands. Such hypothesis would be correct if the beams were bonded. However, the prestressing strands were not bonded to the concrete resulting in the transfer of strain to the strands over their entire length rather than over a short distance in the cracked zone.

Therefore, if the strain in the prestressing strand of an unbonded beam is the same as the strain in the prestressing strand of a bonded beam, the total elongation of the strand, the crack width, the depth of the crack, and the strain in the concrete are larger in an unbonded beam than in a bonded beam. Absence of bond is consequently the cause for only one crack developing[1,2] (see Fig. 16).

Ultimate failure was precipitated by crushing of the concrete rather than by rupture of the prestressing steel because of the concentrated strains in the concrete at the critical section due to the large crack that develops in the beam. This crushing of the concrete developed along the second phase of the moment-rotation diagrams (between L_1 and L_2). However, the restraint of the loading head and the action of the prestressing strands did not allow an abrupt failure of the beams. Once the beams were removed from the testing frame, the compressive zone disintegrated (Fig. 17).

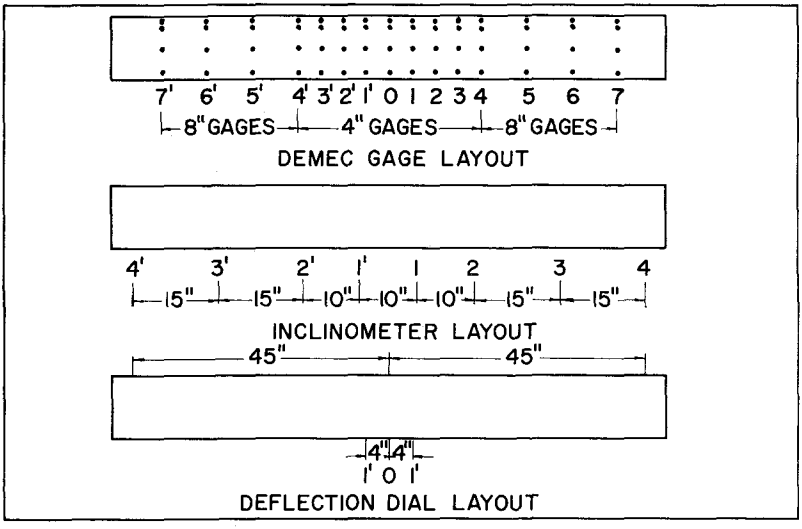

Fig. 8. Beam Instrumentation

The behavior of the beams after the ultimate load was reached, can be described as that of two compression members tied by the prestressing steel acting as a tension member. The arching effect started as the flexure crack developed. High values of localized strain and curvature thus occurred near the loading platten and plastic hinge rotation developed. The equivalent plastic hinge length as determined in this investigation was small, being less than 3 in.

Since the L_1 limit of the beams is defined as the cracking moment limit beyond which a plastic hinge develops, a comparison was made between the observed moment and the computed moment (Table 4). The ratio for the I-beams varied from 0.840 to 1.110 and had a mean value of 0.960; for the T-beams it varied from 0.975 to 1.20 and had a mean of 1.07.

A comparison between computed and observed values of the ultimate moment, beyond the L_2 limit, also showed good agreement. The ratio for the I-beams varied from 0.840 to 1.150 and had a mean value of 0.996. The ratio for the T-beams varied from 0.900 to 1.190 and had a mean value of 1.030.

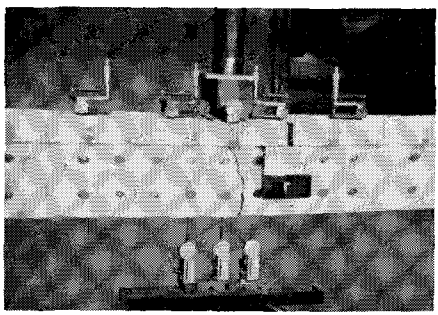

Fig. 9. Typical beam test arrangement

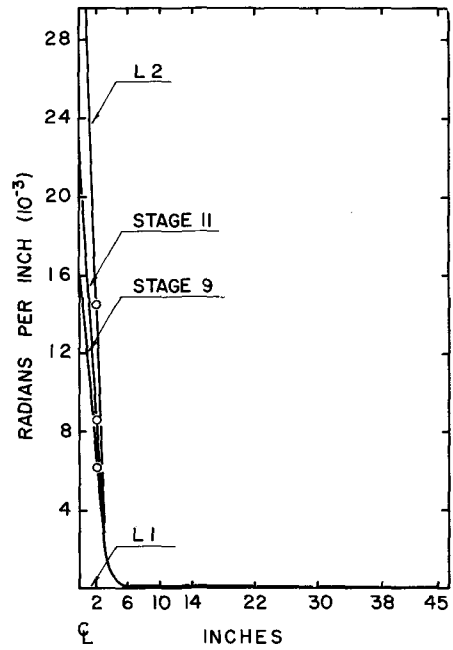

Fig. 10. Typical curvature distribution to failure

Optimum Rectangular Spiral Percentage. The rotation at the L_1 limit for the beams was the sum of the negative rotation due to the prestressing force and the positive rotation due to the actual loading. Variations in rotations for the various beams were due to the prestress slippage at the anchorages during the initial stages of loading.

Limit design of prestressed concrete structures applies to the zones beyond the L_1 stage, namely beyond the cracking load. Thus, the magnitude of the plastic portion of the total rotation determines the degree of ductility of the member or system.

The contribution to increased ductility by the use of rectangular spiral binders in this investigation is given in Fig. 18 relating the magnitude of plastic rotation to the spiral percentage p''. This plot shows that there is an increase in inelastic rotation capa-

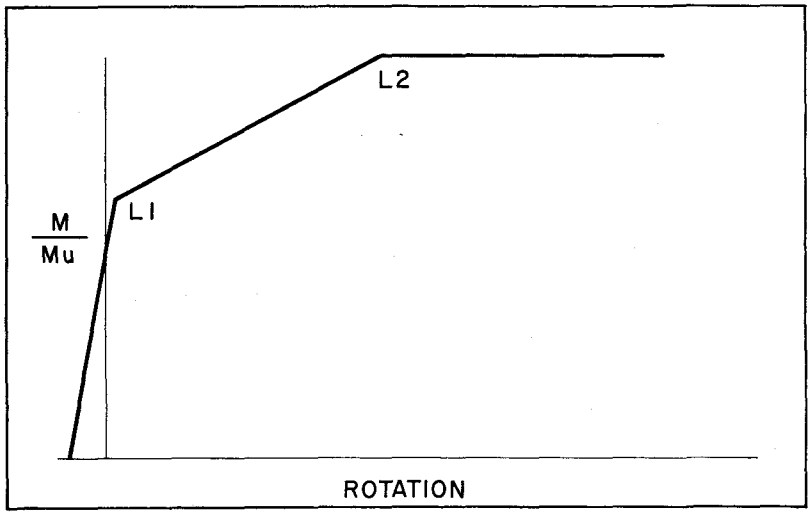

Fig. 11. Idealized moment-rotation diagram

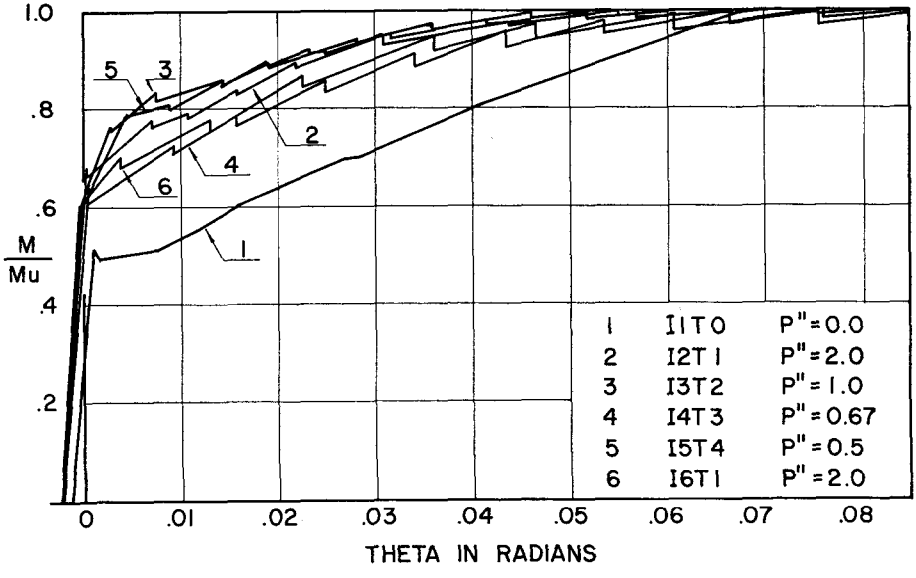

Fig. 12. Moment-rotation diagrams for I-beams

bility with increase in the percentage of spiral binders. This increase is caused by the confinement of the compression zone at the critical section, permitting the compressive block to sustain larger strains and, consequently, larger plastic rotations.

At low percentage p'' up to 1.0 percent the increase in plastic rotation was very small. At 2.0 percent the effect of the spirals on the magnitude of plastic rotation became more pronounced. The plot tends to

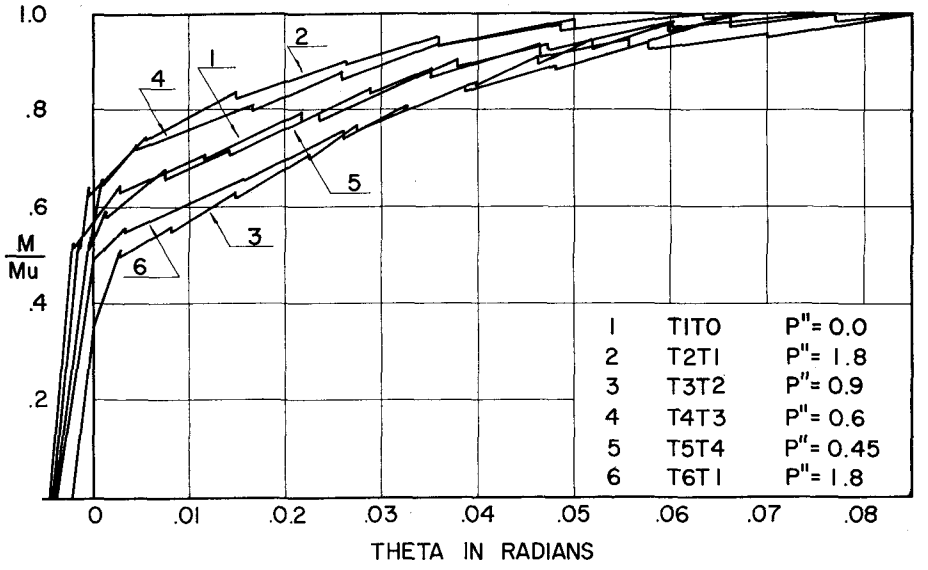

Fig. 13. Moment-rotation diagrams for T-beams

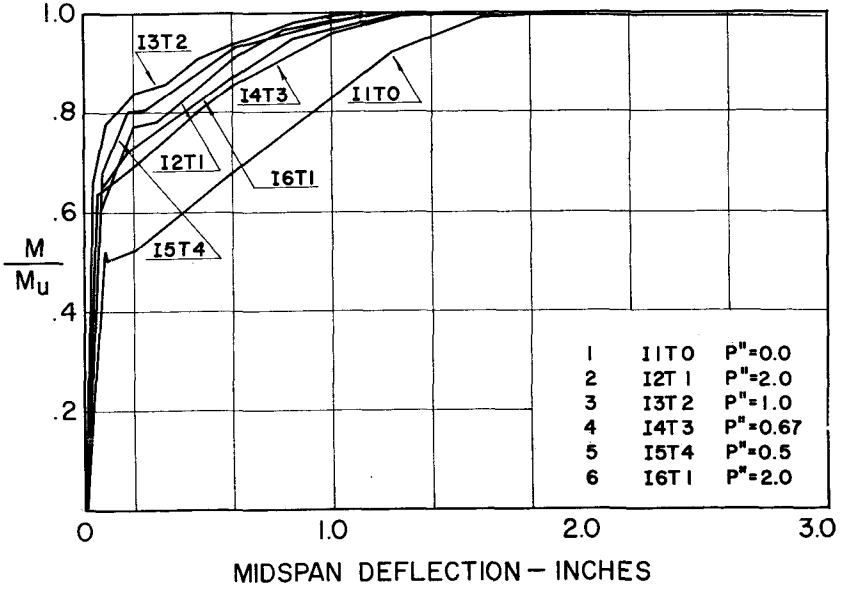

Fig. 14. Moment-deflection diagrams for I-beams

become horizontally asymptotic beyond a value of 2 percent. Continued increase in the percentage p'' would not increase the plastic rotation capability indefinitely. An optimum percentage of spiral binders not too far in excess of 2 percent seems to exist as shown in these tests. Beyond

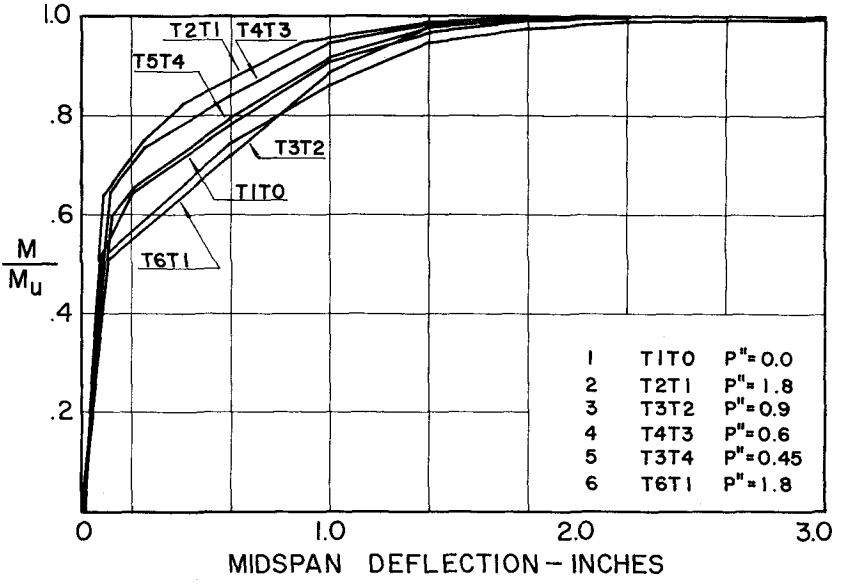

Fig. 15. Moment-deflection diagrams for T-beams

such an optimum, a decrease in plastic rotation capability due to stress concentration can be expected, apart from economic and other practical considerations. Further tests, however, are recommended using p'' values of 2.5 and 3.0 percent to establish precisely the limiting asymptotic value for spiral binder percentages.

CONCLUSIONS

1. Unbonded post-tensioned flanged beams can develop plastic hinges capable of undergoing large magnitudes of rotation.
2. Rotations of unbonded sections can be improved with use of rectangular spiral binders which serve also as shear reinforcement.

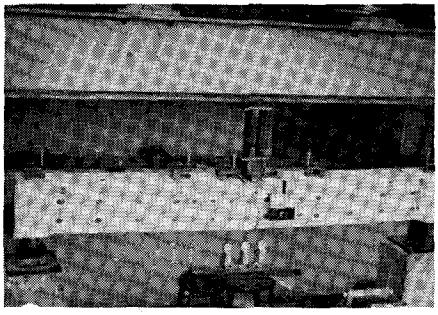
Fig. 16. A T-beam at loading stage 7

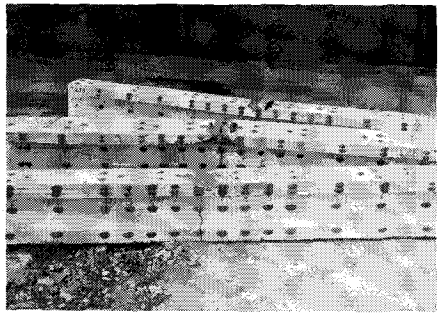
Fig. 17. Top compression fibers at failure

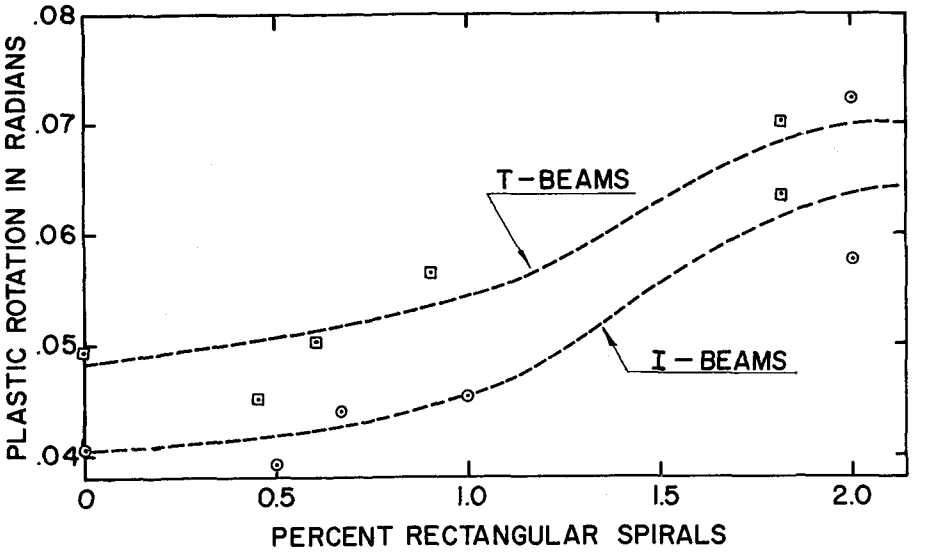

Fig. 18. Plastic rotation vs. rectangular spiral percentage

3. The effect of the spiral binders on the plastic rotation capacity is very limited for binder percentages up to 1.0 percent. At 2.0 per cent, their effect becomes more pronounced permitting a rotation in excess of 0.07 radians.
4. An optimum percentage of spiral binders not much in excess of 2.0 percent seems to exist. Further tests are needed on unbonded beams using spiral percentages of 2.5 to 3.0 to determine more precisely their optimum effect on the plastic rotation capability of the hinges.

ACKNOWLEDGMENT

The authors wish to thank the CF&I Corporation and their Chief Engineer, Mr. Kent Preston, for the prestressing steel used in this investigation. This investigation was conducted at the Concrete Research Laboratories of the Department of Civil Engineering of Rutgers University, and the author's thanks go to Dr. M. L. Granstrom, Chairman, for his support.

REFERENCES

1. Janney, J. R., Hognestad, E. and McHenry, D., "Ultimate Flexural Strength of Prestressed and Conventionally Reinforced Concrete Beams" *Journal of the American Concrete Institute*, Vol. 27, No. 6, Feb. 1956, pp. 601-620.
2. Baker, A. L. L., "The Ultimate Load Theory Applied to the Design of Reinforced and Prestressed Concrete Frames," Concrete Publications, London, 1956, pp. 1-87.
3. Salek, F., "Moment-Rotation Characteristics of Prestressed Post-Tensioned Unbonded Concrete I- and T-Beams," M. S. Thesis, Rutgers University, May 1967, 203 pp.

Discussion of this paper is invited. Please forward your discussion to PCI Headquarters before February 1 to permit publication in the April 1969 issue of the PCI JOURNAL.